NJC

Accepted Manuscript

This is an *Accepted Manuscript*, which has been through the Royal Society of Chemistry peer review process and has been accepted for publication.

Accepted Manuscripts are published online shortly after acceptance, before technical editing, formatting and proof reading. Using this free service, authors can make their results available to the community, in citable form, before we publish the edited article. We will replace this *Accepted Manuscript* with the edited and formatted *Advance Article* as soon as it is available.

You can find more information about *Accepted Manuscripts* in the Information for Authors.

Please note that technical editing may introduce minor changes to the text and/or graphics, which may alter content. The journal's standard Terms & Conditions and the Ethical guidelines still apply. In no event shall the Royal Society of Chemistry be held responsible for any errors or omissions in this *Accepted Manuscript* or any consequences arising from the use of any information it contains.

ROYAL SOCIETY OF CHEMISTRY

www.rsc.org/njc

NJC

RSCPublishing

ARTICLE

Chiral Assembly and Plasmonic Response of Silver Nanoparticles in Three-dimensional Blue-phase Nanostructure Template

Cite this: DOI: 10.1039/xoxxoooooox

Received ooth January 2012,
Accepted ooth January 2012

DOI: 10.1039/xoxxoooooox

www.rsc.org/

Yang Shi, Jun Mo, Jie Wei* and Jinbao Guo*

In this study, we report a new kind of chiral hybrid material which was prepared through three-dimensional (3D) assembly of silver nanoparticles (Ag NPs) into a 3D blue-phase (BP) polymer nanostructure template by in situ reduction of silver nitrate. A feature signal at Ag NPs plasmonic wavelengths could be found in the circular dichroism spectra after Ag NPs assembly within the 3D BP template due to the localized surface plasmon resonance of Ag NPs. Additionally, the chiral hybrid material not only has a sensitive response on the different amount of Ag NPs but also exhibits pronounced sensitivity to the different surrounding dielectric environment. This kind of chiroptical hybrid materials can be valuable in a wide range of applications such as refractive sensor, protein inspection and other biomedical fields.

Introduction

Blue phases (BPs) of liquid crystals (LCs) are of great current interests due to their potential for the application in optical and display fields and also their analogous topological structures in condensed matter systems.[1-6] It is well known that BPs form in high chiral liquid crystal (LC) system and could be classified into three thermodynamically distinct BPs (BP I, BP II and BP III) according to their different spatial orientation.[7-11] BPs could be considered as a stack of double twist cylinders (DTC), in which neighboring LC molecules twist slightly to each other to constitute a helicoidal twist. However, molecular orientations cannot extend smoothly in the space between the cylinders, forming a network of disclinations. At the cores of disclinations, orientational order is reduced, so BPs are usually only one or two degrees that are close to isotropic phase. These spaces of molecular misalignment are unfavorable for the stability of BPs, but instead make it possible to use BPs as a 3D template.[12-14] Ravnik et al.[13] presented extensive computer modeling to demonstrate that colloidal particles can self-assemble into stable 3D periodic structures within BPs as shown in Figure 1A. Meanwhile, polymer network or nanoparticles occupied the disclinations lattice is of great benefit to the stabilization of BPs. The reason is that they can replace part of this energetically costly region and lower the overall energy of the LCs system. In particular, in polymer stabilized BPs, the polymer network provides a 3D self-assembled periodic porous nanostructure template as a result of the disclinations occupied by polymer chains. For example, by the use of wash-out/refill method, also demonstrated by us in polymer stabilized cholesteric LC system,[15] Castles et al.[14] demonstrated thermal stability of BPs in a wider temperature range by refilling 3D BP polymer template with achiral nematic LCs. All these studies have enriched the potential applications of BP 3D topological structures.

In this paper, we report a novel strategy that combines the assembly of metal nanoparticles (NPs) and BP 3D topological structures. As is well known that, metal NPs assembled in chiral environments can show optically active absorption effects over a narrow spectral range in the circular dichroism (CD) spectra because of localized surface plasmon resonance (LSPR).[16-23] Here, Ag NPs can assemble into 3D periodic structure through *in situ* reduction of $AgNO_3$ within a self-assembled 3D nanostructures by polymer templating blue phase I (Figure 1B), which is different from the aforementioned assembly of colloidal particles in the bulk BPs (Figure 1A). By comparing this kind of hybrid materials with the 3D BP polymer template, we find that the resulting architecture exhibits a pronounced circular dichroism signal at Ag plasmonic wavelengths due to the chiral organization of Ag NPs inside of 3D BP template. The improved optical CD allowed us to use these materials in refractive sensor, protein inspection and other biomedical fields.[24-32]

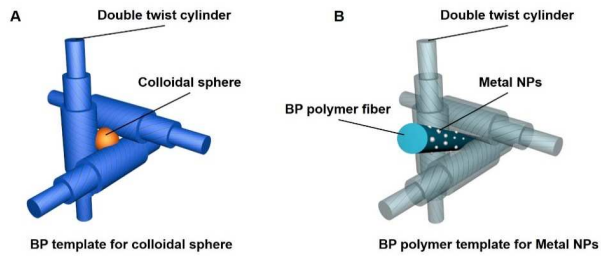

Figure 1. (A) Bulk BPs for the assembly of colloidal spheres, (B) BP polymer template for the assembly of metal NPs.

Experimental Section

Materials

In this study, 4-cyano 4'-4-octylbiphenyl (8CB, Slichem Liquid Crystal Material Co., Ltd), 4-((6-(acryloyloxy)hexyl)oxy)benzoic acid (mono-functional acid, MF-acid), 2-methyl-1,4-phenylene bis(4-((6-(acryloyloxy)hexyl)oxy)benzoate) (diacrylate nematic monomer, C6M)[33], 2-methylbutyl-4-hydroxybiphenyl-40-[6-(acryloyloxy)hexyloxy] benzoic carboxylate (mono-functional liquid crystalline monomer, MF-LCM)[10, 34], 2,5-bis-[40-(hexyloxy)-phenyl-4-carbonyl]-1,4,3,6-dianhydride-D-sorbitol, [chiral dopant (CD), ISO(C6OBA)$_2$][35] and photoinitiator, 2,2-dimethoxy-2-phenyl-acetophenone (Irgacure 651, TCI Co. Ltd.) were used. The chemical structures of all materials used in this study was shown in Figure 2.

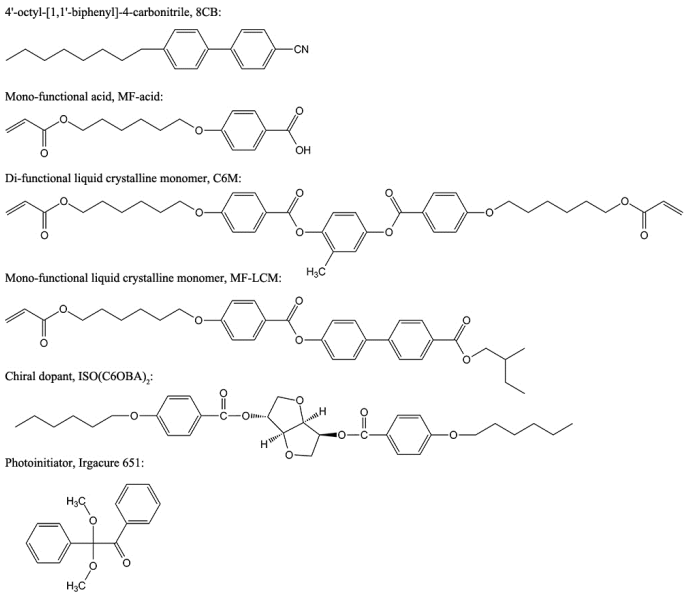

Figure 2. Chemical structures of the materials used in this study.

Measurements

CD and UV-vis absorption spectra were recorded on a JASCO J810 spectrometer and a JASCO V550 spectrometer, respectively. The POM images were observed by a polarizing light microscope (POM) (Leica DM2500) with a hot stage calibrated to an accuracy of ±0.1 °C (Linkam, THMS-600). UV irradiation experiments were performed with a Spectroline ROLENCE-100UV lamp (range 250–500 nm with a maximum at 365 nm). SEM images were obtained using JEOL JSM-7600F, and TEM observations were obtained using JEOL-2100. A CCD camera (Canon EOS 600D) was used for the photographs of the samples.

Preparation of Ag NPs 3D BP polymer template hybrid materials

The 3D free-standing polymer template with nanoscale features which retains the chiral 3D structure of BP I without any chiral molecules was fabricated at first. The schematic diagrams of the preparation process were shown in Figure 3. First, the LC mixture was filled between two glass substrates without orientation after proportionally mixed each components, the LC mixture self-assembled to BPI during cooling from the isotropic phase, and the thickness of the samples was controlled by 10 μm polyethylene spacer (Figure 3A). Then, as shown in Figure 3B, the cell was illuminated with ultraviolet light (365 nm, 3mW/cm^2) to polymerize for 5 min at 26.5 °C. In this process, the polymerized components moved to the disclinations and polymerized to polymer chains in disclination lines to freeze 3D BP periodic structure. After that, we used washout method to prepare BP polymer template, the cell was soaked in cyclohexane for 24 h and THF for 4 h respectively to wash out the LC host, chiral dopant and any remaining unpolymerized functional material/photoinitiator. After dried in air, the BP template was obtained. In the next step, to reduce Ag NPs within the BP template, the BP template was soaked in $AgNO_3$ solution which was dissolved in water and ethanol [V (EtOH) : V (H_2O) = 2 : 1] over 24 h, then after drying, we immersed it into a freshly prepared $NaBH_4$ solution [V (EtOH) : V (H_2O) = 2 : 1] for 3 min to reduce Ag^+ to Ag^0. The addition of ethanol could develop the penetration of solutions into the polymer network because our BP polymer template had a good compatibility with ethanol. The nanoparticle size and distribution of Ag NPs were controlled by the reduction time in $NaBH_4$ solution. Here, two $AgNO_3$ concentrations of 10mM and 50mM were used, and the concentrations of $NaBH_4$ solutions were doubled to 20mM and 100mM, respectively. At last, the chiral hybrid materials were prepared after drying.

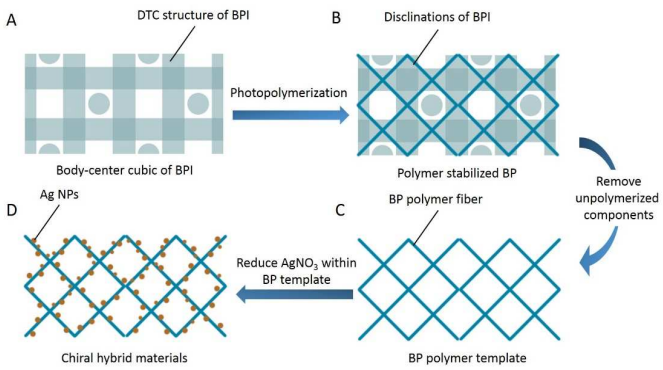

Figure 3. The schematic diagrams of the preparation process of Ag NPs 3D BP polymer template hybrid materials.

Results and Discussion

3D BP polymer template

In order to fabricate the 3D BP polymer template, 8CB was used as the host LCs, MF-acid, C6M and MF-LCM were used to form BPs and BP polymer template. It is worth mentioning that the addition of MF-acid is to enhance the hydrophilic nature of the polymer fibers and further to induce the assembly of Ag NPs on the fibers. ISO(C6OBA)$_2$ is the chiral dopant to produce chirality for the system and Irgacure 651 is the photoinitiator to initiate polymerization. Premixture was composed of 81.9 wt% 8CB, 3 wt% MF acid, 2 wt% C6M, 4.6 wt% MF-LCM, 8.5 wt% ISO(C6OBA)$_2$, and 2 wt% by weight of polymerized monomers of Irgacure 651.

Before polymerization, we chose an appropriate temperature for polymerization. Here, the phase states and corresponding transition temperatures for LC mixtures were determined by POM with heating and cooling rate as 0.5 °C min^{-1}. We could observe that the platelet textures with various colors of BPI are clear and homogeneous in POM during the cooling process. At 31.0 °C, the platelets appeared, then grew up gradually and covered the whole area of the cell at 26.5°C and the cell appeared a shiny blue, as shown in Figure 4A. When the cell temperature approaches 24.0 °C, cholesteric phase covered the whole cell instead of BP platelets. Herein, we chose 26.5 °C as polymerization temperature to freeze BPI structure during the polymerization process.

The samples were illuminated with a UV light (365 nm, 3mW/cm^2) for polymerization induced phase separation (PIPS). During the polymerization, polymerized components initially aggregate as polymer spheres and move to the defect region of LC to finally form polymer fibers.[36] Figure 4 shows the POM images and digital photos of polymer stabilized BP samples before polymerization, after polymerization and wash-out process, respectively. As shown in Figure 4B, the POM image and digital photo show that BPI structure was frozen until room temperature after polymerization. Finally, by using wash-out method, the BP 3D template was prepared as shown in Figure 4C. What's more, the POM image suggests that the BP polymer template was isotropic as shown in Figure 4C. In this case, the effect of birefringence on the CD measurement is also eliminated. We also check whether there exists linear polarization effect in BP template observed by POM with rotating only one polarizer. The intensity of transmission light through BP template is almost no change when the polarizer is rotated from 0° to 180°. Therefore, the CD measurement can not be influenced by linear polarization effect.

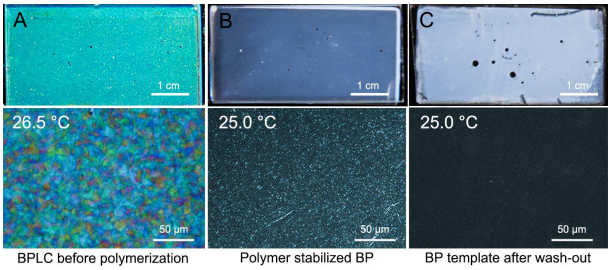

Figure 4. The POM images and digital photos of (A) BPLC before polymerization, (B) polymer stabilized BP and (C) BP template after wash-out.

The disclination lines of the BPI are ordered due to the cubic symmetry,[37] therefore the BP polymer fiber which occupied the disclination lines could form a periodic network as shown in Figure 5B after PIPS process. Our experimental results demonstrate that, as shown of SEM image in Figure 5A, the BP polymer template has a basically 3D regular structure, in which the average size of porous structures is several hundred nanometers that are consistent with the periodicity of the lattice produced in the BPs. This periodic network plays an important role on retaining the optical activity of BPs.[14] However, we also note that, the complexity of the polymerization and sample preparation process may bring the deviations between the actual polymer network and theoretical structure. For example, the temperature fluctuation was caused by UV radiation during polymerization process and the polymer network was slightly damaged in the wash-out process. However, the formation of the pores in BP template is an important evidence, which allows us to confirm the polymer network is produced from BP cubic structure and retains the optical activity of BPs.[14]

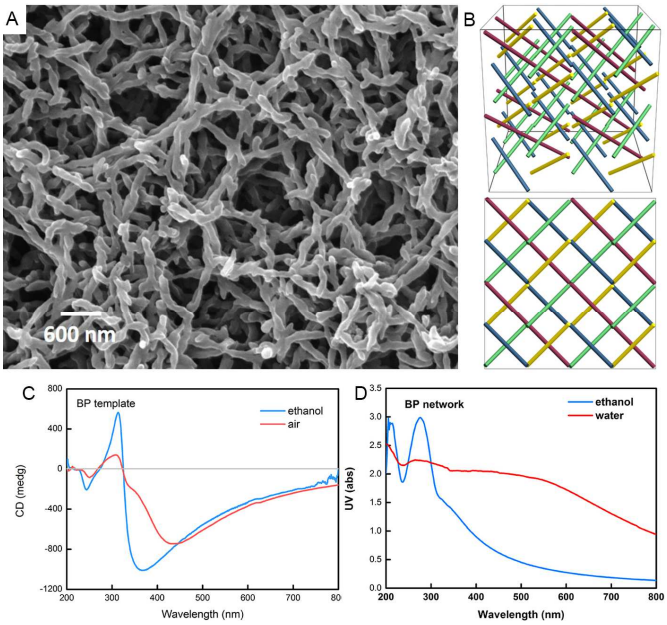

Figure 5. (A) SEM image of BP polymer template; (B) 3D arrangement and 2D projection of the disclination network in BPI, CD (C) and UV-Vis (D) spectra of BP template in ethanol (blue) and air (red).

Figure 5C-D show the CD and UV-Vis spectra of the BP template in air and ethanol. We find some differences of the CD spectra between them as shown in Figure 5C. The CD spectra of BP template in air shows a positive cotton effect at 308 nm and negative cotton effect at 249 and 433 nm with crossover at 268 and 325 nm. While the CD spectra of BP template in ethanol exhibits a positive cotton effect at 313 nm and negative cotton effect at 243 and 368 nm with crossover at 272 and 325 nm. Meanwhile, from the UV-Vis spectra, shown in Figure 5D, the BP template exhibits lower transmission intensity in air than that in ethanol in the visible region, which agrees well with the CD results for the BP template in air and ethanol. These results may be due to that the BP template has a porous structure at the interface between the polymer network and air. However, when the porous structure of the BP template was full of ethanol, the transmission of the template has a great improvement owing to the match of the refractive index between two mediums. Actually, this porous structure has little influence on the position and intensity of CD signals as we measured many samples whose CD spectra were basically consistent. Here we note that the fact that the BP template has a good compatibility with ethanol gives us a chance to make Ag^+ enter into the nanoporous to achieve the objective that Ag NPs can assemble into BP polymer template.

Optical activity of BP template loaded with Ag NPs

After loaded with Ag NPs, the hybrid material demonstrated a special optical activity. By comparing with the CD spectra of the pure BP template soaked in ethanol (Figure 5C), CD spectra of the BP template loaded with Ag NPs (Figure 6A and C) exhibits strong features signal at 412 nm, featuring a strong intensity change after loading Ag NPs. Meanwhile, UV-Vis spectra of BP template loaded with Ag NPs shows a peak at around 400 nm assigned to the localized surface plasmon resonance of Ag NPs (Figure 6B). Additionally, the intensity of the sample prepared by using 50mM $AgNO_3$ (high concentration) solution is more obvious than that of the sample prepared by using 10mM $AgNO_3$ (low concentration) solution in Figure 6A. This may be due to that more Ag NPs within the BP template from high concentration of Ag^+ decreases the distance between the NPs which induces the difference of LSPR peaks in the CD and UV-Vis spectra[20] (Figure 6A and B) as demonstrated later.

The effect of the change of refractive index (dielectric constant) of surrounding environment on the LSPRs of our chiral hybrid material was further investigated. By comparing the chiral hybrid material soaked in ethanol and water, the feature CD signals have a blue-shift moving from 412 nm to 392 nm (Figure 6C) obviously. While the shift of LSPR absorbance peaks in UV-Vis spectra in two solvents was very little (Figure 6D). Therefore, a large blue-shift observed in the CD spectra suggests that the optical activity is more sensitive than the movement of the LSPR absorbance peaks to environment changes, showing that this kind of chiral assembly Ag NPs hybrid material could be used in biological and physical fields.

Feature CD signals appeared at plasmonic wavelength of Ag NPs means the chiral organization of the Ag NPs was formed inside the BP template after Ag NPs were reduced within the BP template. The chirality may come from the periodic nanostructure of BP template or come from the individual Ag NPs. If the chirality come from BP template, the hybrid materials could be effective only when the Ag NPs assembled within BP template. To get a clear understanding about this, the Ag NPs were eluted by ethanol from the two hybrid samples (high and low concentrations) respectively. The CD and UV-Vis spectra were measured and shown in Figure 7. The LSPR absorbance peaks of Ag NPs could be clearly observed in both UV-Vis spectra, however, there were no any CD signals in both CD spectra.

Our experimental results demonstrate that, there is no chiral optical activity in the individual NPs and the chirality of Ag NPs stems from the 3D BP template. As is well known, a chiral driving force is necessary in a chiral system although there was no chiral molecule or groups in our BP template.[38] However, the chiral dopants provided chiral force to induce the formation of double twist arrangement of achiral molecule before polymerization. After photopolymerization and removal of the non-reactive components, this chiral twist structure is memorized by the polymer network as a periodic porous structure, yielding the required chiral driving force for the hybrid material. Therefore, the chirality of BP template is originated from the periodicity of the polymer network rather than from any chiral molecular-structure. On the other hand, BPLC could be regarded as a kind of 3D bi-chiral photonic crystals,[39,40] where polymer fibers arranged along the three orthogonal axes of a cubic lattice to provide a chiral periodic structure. Furthermore, we note that the feature CD signal is due to plasmon-plasmon Coulombic interactions between neighboring Ag NPs inside of the 3D BP template, which is different from CD signals that are induced from chiral ligand-stabilized nanoparticles. According to our above elution experimental, no CD signals could be detected in this condition, which means the feature CD signal can be induced only when the chiral organization of the Ag NPs is formed in BP template not just the electronic interaction of nanoparticles is provided.

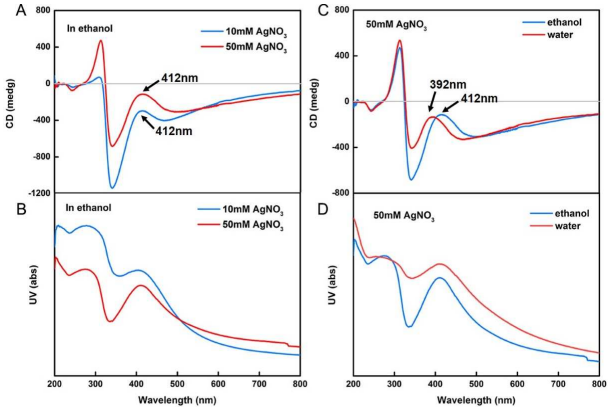

Figure 6. CD (A) and UV-Vis (B) spectra of BP template loaded with different concentration Ag NPs, as low concentration (blue) and high concentration (red); CD (C) and UV-Vis (D) spectra of BP template loaded with high concentration Ag NPs in ethanol (blue) and water (red).

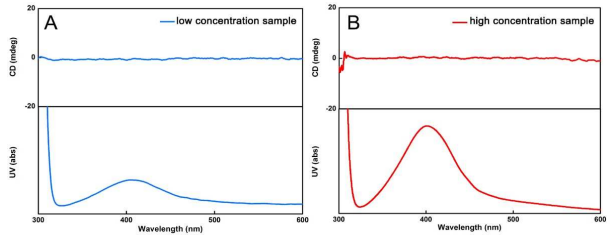

Figure 7. CD and UV-Vis spectrum of eluted Ag NPs as low concentration (A) and high concentration (B).

Distribution of Ag NPs in BP template

When Ag NPs were reduced within the template, Ag NPs may exist in three conditions: (1) loading on the surface of polymer fibers, (2) existing inside the pores and (3) separated from the BP template. Here, the first condition could be regarded as Ag NPs assembled with BP template well. Actually, these three conditions had all appeared in our study and there were nearly no feature CD signals appearing when the chiral hybrid material was measured in the latter two conditions. In order to get a good distribution of Ag NPs inside the polymer network, we have tried many experimental ways. For example, we have tried hydroquinone (HQ) as reductant and polyvinylpyrrolidone (PVP) as protectant to reduce $AgNO_3$ to form Ag NPs. But the Ag NPs have a wide size distribution and tend to be aggregation inside the polymer network. In addition, the Ag NPs get into the polymer network difficultly due to the high viscosity of the PVP. So we chose $NaBH_4$ to reduce $AgNO_3$ without protectant because the adsorption of borohydride can stabilize silver nanoparticles by providing a particle surface charge to avoid aggregation.[41,42] The Ag NPs which locate the surface of BP polymer fibers form a metal-dielectric interface. When electromagnetic (EM) wave propagate along the interface, the EM wave induces a coherent oscillation of surface conduction electrons to excite the LSPR of Ag NPs. Because of the chiral characteristics of the 3D periodic structure in BP template, a feature signal at plasmoic wavelength of Ag NPs could be detected in CD spectra. The key factor to control the distribution of Ag NPs in BP template is the reduction time. In our study, Ag NPs will become large aggregates and divided from the BP template if reduction time is too long, and the best time is 3 min. The SEM and TEM images of Ag NPs-loaded BP template as reduced for 3 min were shown in Figure 8B, C and D. It could be found the Ag NPs loaded on the surface of the polymer fibers, and no Ag NPs were in pores or separated from the template. Compared Figure 8B and C, we can find the interparticle spacing has been decreased in Figure 8C due to the increase in the amount of nanoparticles as mentioned above. As shown in Figure 8D, the size of Ag NPs with the diameter of ranging from 10 to 20 nm just appeared on the surface of polymer fibers, which means that Ag NPs assembled within BP template well. Although the arrangement of Ag NPs seems random and disordered, this state does not influence the CD spectrum and the feature CD signal remains pronounced.[43] What's more, it should be noted that reducing Ag NPs within BP template play an important role in chiral organization, no CD signals could be detected if we just doped preformed Ag NPs into the BP template.

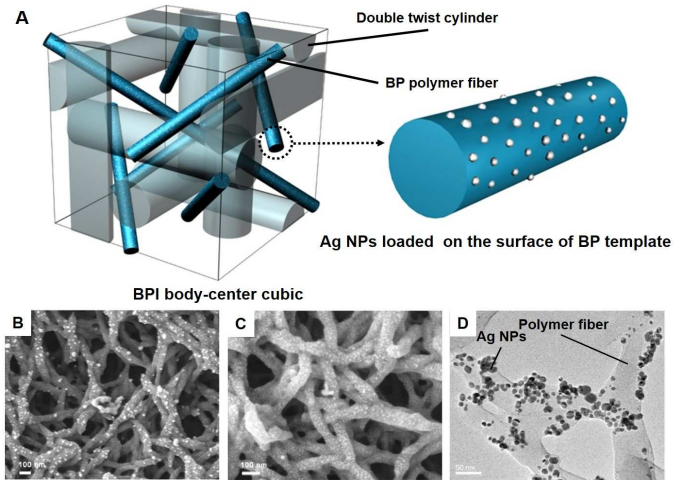

Figure 8. (A) Schematic diagram of BP polymer template for the assembly of Ag NPs. The BP polymer fibers occupied the disclination for the reduction of Ag NPs on the surface of the fiber. SEM images of Ag NPs assembly within the BP template in low concentration (B) and high concentration (C) and (D) TEM image of BP template for the assembly of Ag NPs (low concentration).

Conclusions

To summarize, we propose a new approach toward assembled chiral 3D hybrid materials using Ag NPs and chiral 3D polymer BP template. The results show the hybrid architectures with Ag NPs exhibit optical activities in the vicinity of the LSPR of the Ag NPs as well as the capacity for responding to the dielectric environment. We confirmed this optical activity stems from the BP template rather than from a property of the individual Ag NPs. This strategy could be extended to fabricate other chiral plasmonic hybrid structure by selecting other metal ions or semiconducting nanoparticles. The sensitivity to the dielectric environments of these chiroptical hybrid materials makes them promising applications for sensing and other related fields.

Acknowledgements

This research was supported by National Natural Science Foundation (Grant No. 51373013, 51173013, 50903004) and Beijing Young Talents Plan (YETP0489).

College of Materials Science and Engineering, Beijing University of Chemical Technology, Beijing 100029, P. R. China
E-mail: guojb@mail.buct.edu.cn
weij@mail.buct.edu.cn

Notes and references

1 H. J. Coles and M. N. Pivnenko, *Nature*, 2005, **436**, 997-1000.
2 W. Cao, A. Munoz, P. Palffy-Muhoray and B. Taheri, *Nat. Mater.*, 2002, **1**, 111-113.
3 H. Kikuchi, M. Yokota, Y. Hisakado, H. Yang and T. Kajiyama, *Nat. Mater.*, 2002, **1**, 64-68.
4 S. Yokoyama, S. Mashiko, H. Kikuchi, K. Uchida and T. Nagamura, *Adv. Mater.*, 2006, **18**, 48-51.
5 K. Higashiguchi, K. Yasui and H. Kikuchi, *J. Am. Chem. Soc.*, 2008, **130**, 6326-6327.
6 L. Wang, W. He, X. Xiao, F. Meng, Y. Zhang, P. Yang, L. Wang, J. Xiao, H. Yang and Y. Lu, *Small*, 2012, **8**, 2189-2193.
7 B. Li, W. He, L. Wang, X. Xiao and H. Yang, *Soft Matter*, 2013, **9**, 1172-1177.
8 H. Stegemeyer, T. H. Blümel, K. Hiltrop, H. Onusseit and F. Porsch, *Liq. Cryst.,* 1986, **1**, 3-28.
9 D. C. Wright and N. D. Mermin, *Rev. Mod. Phys.*, 1989, **61**, 385-432.
10 J. Guo, Y. Shi, X. Han, O. Jin, J. Wei and H. Yang, *J. Mater. Chem. C*, 2013, **1**, 947-957.
11 Y. Shi, X. Wang, J. Wei, H. Yang and J. Guo, *Soft Matter*, 2013, **9**, 10186-10195.
12 O. D. Lavrentovich, *Proc. Natl. Acad. Sci. USA*, 2011, **108**, 5143-5144.
13 M. Ravnik, G. P. Alexander, J. M. Yeomans and S. Zumer, *Proc. Natl. Acad. Sci. USA*, 2011, **108**, 5188-5192.
14 F. Castles, F. V. Day, S. M. Morris, D. H. Ko, D. J. Gardiner, M. M. Qasim, S. Nosheen, P. J. Hands, S. S. Choi, R. H. Friend and H. J. Coles, *Nat. Mater.*, 2012, **11**, 599-603.
15 J. Guo, H. Cao, J. Wei, D. Zhang, F. Liu, G. Pan, D. Zhao, W. He and H. Yang, *Appl. Phys. Lett.*, 2008, **93**, 201901.
16 H. Yao, K. Miki, N. Nishida, A. Sasaki and K. Kimura, *J. Am. Chem. Soc.*, 2005, **127**, 15536-15543.
17 M. E. Layani, A. Ben Moshe, M. Varenik, O. Regev, H. Zhang, A. O. Govorov and G. Markovich, *J. Phys. Chem. C,* 2013, **117**, 22240-22244.
18 H. Qi, K. E. Shopsowitz, W. Y. Hamad and M. J. MacLachlan, *J. Am. Chem. Soc.*, 2011, **133**, 3728-3731.
19 Y. Li and M. Liu, *Chem. Commun.*, 2008, **43**, 5571-5573.
20 J. A. Kelly, K. E. Shopsowitz, J. M. Ahn, W. Y. Hamad and M. J. MacLachlan, *Langmuir*, 2012, **28**, 17256-17262.
21 A. O. Govorov and Z. Fan, *Chemphyschem*, 2012, **13**, 2551-2560.
22 G. D. Lilly, A. Agarwal, S. Srivastava and N. A. Kotov, *Small*, 2011, **7**, 2004-2009.
23 A. O. Govorov, Y. K. Gun'ko, J. M. Slocik, V. A. Gérard, Z. Fan and R. R. Naik, *J. Mater. Chem.*, 2011, **21**, 16806-16818.
24 J. Xie, Y. Duan and S. Che, *Adv. Funct. Mater.*, 2012, **22**, 3784-3792.
25 A. Guerrero-Martinez, B. Auguie, J. L. Alonso-Gomez, Z. Dzolic, S. Gomez-Grana, M. Zinic, M. M. Cid and L. M. Liz-Marzan, *Angew. Chem. Int. Ed.*, 2011, **50**, 5499-5503.
26 B. Kim, S. J. Choi, S. H. Han, K. Y. Choi and Y. B. Lim, *Chem. Commun.*, 2013, **49**, 7617-7619.
27 A. Ben-Moshe, B. M. Maoz, A. O. Govorov and G. Markovich, *Chem. Soc. Rev.*, 2013, **42**, 7028-7041.
28 A. Querejeta-Fernandez, G. Chauve, M. Methot, J. Bouchard and E. Kumacheva, *J. Am. Chem. Soc.*, 2014, **136**, 4788-4793.
29 C. Gautier and T. Bürgi, *J. Am. Chem. Soc.*, 2006, **128**, 11079-11087.
30 G. Shemer, O. Krichevski, G. Markovich, T. Molotsky, I. Lubitz and A. B. Kotlyar, *J. Am. Chem. Soc.*, 2006, **128**, 11006-11007.
31 A. Guerrero-Martínez, J. L. Alonso-Gómez, B. Auguié, M. M. Cid and L. M. Liz-Marzán, *Nano Today*, 2011, **6**, 381-400.
32 A. Kuzyk, R. Schreiber, Z. Fan, G. Pardatscher, E.-M. Roller, A. Hogele, F. C. Simmel, A. O. Govorov and T. Liedl, *Nature*, 2012, **483**, 311-314.
33 D. J. Broer, J. Boven, G. N. Mol and G. Challa, *Makromol. Chem.*, 1989, **190**, 2255-2268.
34 W. Y. Zheng and P. T. Hammond, *Macromol. Rapid. Commun.*, 1996, **17**, 813-824.
35 V. Vill, F. Fischer and J. Thiem, Zeitschrift für Naturforschung. *A: A Phys. Sci.*, 1988, **43**, 1119-1125.
36 D. Voloschenko, O. Pishnyak, S. Shiyanovskii and O. Lavrentovich, *Phys. Rev. E*, 2002, **65**, 060701.
37 M. Ravnik, J.-i. Fukuda, J. M. Yeomans and S. Žumer, *Soft Matter*, 2011, **7**, 10144-10150.
38 Y. Sawa, F. Ye, K. Urayama, T. Takigawa, V. Gimenez-Pinto, R. L. Selinger and J. V. Selinger, *Proc. Natl. Acad. Sci. USA*, 2011, **108**, 6364-6368.
39 S. S. Oh, A. Demetriadou, S. Wuestner and O. Hess, *Adv. Mater.*, 2013, **25**, 612-617.
40 G. von Freymann, A. Ledermann, M. Thiel, I. Staude, S. Essig, K. Busch and M. Wegener, *Adv. Funct. Mater.*, 2010, **20**, 1038-1052.
41 L. Mulfinger, S. D. Solomon, M. Bahadory, A. V. Jeyarajasingam, S. A. Rutkowsky and C. Boritz, *J. Chem. Edu.*, 2007, **84**, 322-325.
42 A. Zielińska, E. Skwarek, A. Zaleska, M. Gazda and J. Hupka, *Procedia Chem.*, 2009, **1**, 1560-1566.
43 Z. Fan and A. O. Govorov, *J. Phys. Chem. C*, 2011, **115**, 13254-13261.